ACS OMEGA

http://pubs.acs.org/journal/acsodf

Article

Composition–Structure Relationship and Routes of Formation of Blocklike Ferrospheres Produced by Pulverized Combustion of Two Coal Types

Natalia N. Anshits, Elena V. Fomenko, and Alexander G. Anshits*

Cite This: *ACS Omega* 2021, 6, 26004–26015

Read Online

ACCESS | Metrics & More | Article Recommendations

ABSTRACT: The composition–structure relationship of blocklike ferrospheres (FSs) isolated from fly ash produced during the combustion of two different types of coal was studied systematically by scanning electron microscopy coupled with energy-dispersive X-ray spectroscopy. Monoblock globules were shown to consist of large sintered crystallites of Mg, Mn ferrospinel, which are formed from excluded siderite particles containing isomorphic impurities of magnesium and manganese carbonates. The common groups of globules for which the gross composition of polished sections corresponds to the general equations for the relationship of the concentrations $SiO_2 = f(Al_2O_3)$ and $CaO = f(SiO_2)$ were highlighted from FSs of two series. These globules are formed during the thermochemical transformation of associates of siderite, quartz, calcite, and anorthite, which have a silicate modulus of SiO_2/Al_2O_3 equal to 1.18, which corresponds to the coefficients in the general equations of the relationship $SiO_2 = f(Al_2O_3)$. SEM analysis of polished cross-sections of the globules of selected FS groups demonstrates that the crystallite size of ferrospinel decreases, while the content of the glass phase increases with the declining FeO concentration in individual globules. The crystallite size and shape are found to depend on the size of the local melt area where the concentration of spinel-forming oxides is >85 wt %. The observed increase in the glass-phase content is attributed to the broadening of the liquation zone in the $FeO–Fe_2O_3–SiO_2$ system as the oxidative potential increases and to the higher content of $[Fe^{3+}O_2]^-$ and $[Fe^{3+}{}_2O_5]^{4-}$ ferrite complexes in calcium-rich melts.

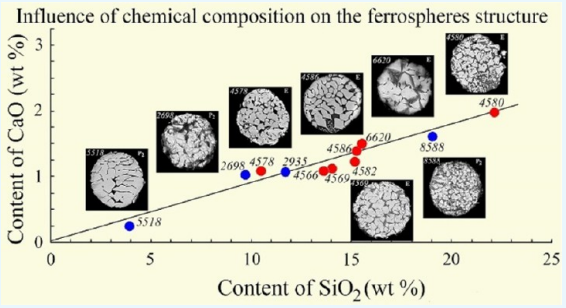

INTRODUCTION

Fly ash from coal-fired power plants mainly consists of the products of decomposition and alteration of mineral matter in coal, as well as small amounts of unburnt carbon.[1−8] The formation of ash particles during pulverized coal combustion involves several thermochemical processes: coalescence of included minerals,[9−11] char fragmentation,[12] and fragmentation of excluded minerals.[13,14] The composition, morphology, and particle size distribution are determined by a combination of the aforementioned processes and depend on the coal combustion conditions and characteristics of the mineral components of coal.[3,6−8,11,15,16]

There has recently been a keen interest among researchers in the production of functional materials based on individual fly ash components, such as adsorbents, catalysts, carriers, ceramic materials, and zeolites.[17−24]

Ferrospheres (FSs) are among the most common components of fly ashes. Due to their magnetic properties, they can be isolated from different ashes in the form of magnetic concentrates (MCs) whose compositions vary widely: Fe_2O_3, 20−88 wt %; SiO_2, 8−40 wt %; Al_2O_3, 3−21 wt %; and CaO, 3−8 wt %.[3,6,25,27] Various Fe-bearing species (mostly including magnetite, hematite, ferrian spinel, Ca and Ca–Mg ferrite spinels, and, to a lesser extent, maghemite, martite, mushketovite, wustite, ilmenite, chromite, Mn ferrite, ferrosilicon, iron hydroxides, and iron silicates) were identified in these MCs.[25−32] Other minerals and phases such as glass, quartz, char, anhydrite gypsum, feldspars, kaolinite, mica, mullite, carbonates, periclase, spinels, and Cr–Ni spinels were also found to be associated with the aforelisted Fe-containing species in MCs.

By using process flow diagrams for separation and deep purification of FS concentrates, which include the granulometric, hydrodynamic, dry, and wet magnetic separation stages, the known ash types can be classified into narrow fractions of FSs having a constant composition (with the Fe_2O_3 content ranging from 30 to 92 wt % and the globule size ranging from 50 to 250 μm[33]) and being characterized by reproducible magnetic

Received: June 2, 2021
Accepted: September 10, 2021
Published: September 29, 2021

properties.[34,35] The compositions of the major components of all the studied narrow fractions of FSs and MCs obtained from 17 power plants in Russia, Ukraine, and Kazakhstan were found to be described by two general linear regression equations: $[SiO_2] = 65.71 - 0.71[Fe_2O_3]$ and $[Al_2O_3] = 24.92 - 0.26[Fe_2O_3]$, with the correlation coefficients of −0.99 and −0.97, respectively. It was also shown that with the increasing iron concentration in the narrow fraction, the main morphological type of FSs changes in the following sequence: porous (spongy), glass-like, fine-grained (dendritic), skeletal−dendritic, and blocklike FSs.[33] The produced FS fractions have the common composition−morphology−microstructure relationship for iron-containing phases; in turn, this suggests that they can be used as functional materials. In particular, narrow fractions of clean FSs separated from industrial coal combustion fly ashes are sufficiently often used as efficient catalysts for deep oxidation,[36,37] oxidative coupling of methane (OCM),[37−39] and thermolysis of heavy oil and petroleum residue[40,41] and as magnetic carriers for isolating recombinant proteins.[42] The properties of microspherical functional materials in each particular case depend on their composition, morphology of globules, crystallite size, and microstructure of active phases. In particular, it is demonstrated that FS narrow fractions from burning brown coal with Fe_2O_3 content (≥89 wt %) include 10% of platelike globules consisting of needlelike crystallites of calcium ferrite,[43] which is the active phase for OCM.[38] FS narrow fractions containing 30−79 wt % Fe_2O_3 from burning coals do not contain platelike FSs. At the same time, they contain a significant number of individual globules of skeletal−dendritic and blocklike structures, including magnesium−aluminium−ferrite spinel,[33] which is the active phase for deep oxidation of methane.[36,37] It is found that the FS narrow fractions sized −0.05 mm with contents of 71.3 and 66.4 wt % of Fe_2O_3 isolated from fly ashes produced by combustion of coals from the Ekibastuz and Kuznetsk basins, respectively, have the maximum activity in the methane deep oxidation reaction.[37] The search for promising sources of narrow FS fractions with a high content of a certain globule type active in a particular process requires a general idea of the pathways for globule formation.

This paper presents the results of a systematic study of the content of FSs of different morphological types and the relationship of the major component composition and structure of individual blocklike FSs separated from the Ekibastuz and Kuznetsk coal fly ash. The aim of this work is the investigation of the features of FS formation routes and the nature of mineral precursors controlling the FS structure.

RESULTS AND DISCUSSION

Combustion of coals of different origins gives rise to FSs of several morphological types. Narrow fractions E−0.05 mm and P_2−0.05 mm isolated from fly ashes produced during the combustion of coal from the Ekibastuz and Kuznetsk basins were used to quantify the different types of globules and study the relationship between the composition of major components and structure of individual blocklike FSs.

Fe_2O_3 (71.32 and 66.38 wt %), SiO_2 (19.20 and 20.70 wt %), and Al_2O_3 (8.39 and 6.62 wt %) are the main components of the −0.05 mm fractions of series E and P_2; their total contents are 98.91 and 93.70 wt %, respectively. The contents of CaO and MgO in the series E fraction (1.96 and 1.01 wt %, respectively) are lower than those for series P_2 (2.94 and 2.82 wt %, respectively). The phase composition of the E−0.05 mm and P_2−0.05 mm fractions includes ferrospinel (45.6 and 52.5 wt %), hematite (4.3 and 7.3 wt %), quartz (2.6 and 2.4 wt %), mullite (2.9 and 0.7 wt %), ε-Fe_2O_3 (2.8 and 2.0 wt %), and an amorphous phase (41.8 and 35.1 wt %). The unit cell parameters a of ferrospinel of the studied fractions are 8.360(1) and 8.368(1) Å, respectively. Unit cell parameters of hematite are a = 5.0302(6) Å and c = 13.729(3) Å for series E and a = 5.0316(4) Å and c = 13.732(2) Å for series P_2 fractions. The reported parameters are much lower than those for the stoichiometric oxides Fe_3O_4 (a = 8.3960 Å) and Fe_2O_3 (a = 5.0356 Å), which indicate that Fe^{2+} and Fe^{3+} cations are partially replaced by Al^{3+} and Mg^{2+} cations having smaller ionic radii. Iron cations are replaced to a greater extent in the E−0.05 mm fraction of FSs than that in the P_2−0.05 mm fraction.[33]

An analysis of the scanning electron microscopy (SEM) images of ∼1400 globules of the P_2−0.05 mm fraction and ∼900 globules of the E−0.05 mm fraction showed that they contain 50 and 64% of skeletal−dendritic FSs; 19 and 11% of blocklike FSs; and 5 and 8% of spongy FSs, respectively. The content of platelike globules in both fractions is <1%. The contents of plerospheres in the analyzed fractions are 7 and 4%, respectively (Figure 1). It should be mentioned that the contents of the

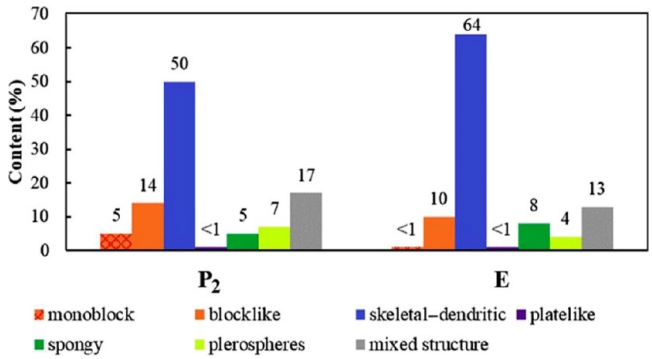

Figure 1. Content of FSs of different morphological types in ashes from the combustion of two types of coal (series P_2 and series E).

aforelisted morphological types in the analyzed fractions differ significantly from those for the previously studied FS fraction isolated from fly ash produced during the combustion of calcium-rich brown coal, which contains no spongy globules, while the contents of blocklike, skeletal−dendritic, and platelike globules are 58, 16, and 10%, respectively.[43,44] The presence of globules with a spongy structure and the absence of platelike globules prove that the structure of FSs depends on mineral precursors in initial coals. In particular, it was shown that platelike FSs are formed during the sequential conversion of the dispersed products of thermal conversion of pyrite and complex Fe, Ca, and Mg humates of initial brown coal.[45] Illite is an aluminosilicate precursor responsible for the structure of skeletal−dendritic globules that are formed during the combustion of bituminous and brown coal. Crystallization of iron aluminosilicate melt droplets giving rise to skeletal−dendritic globules occurs due to the "crystal seed" of Al, Mg ferrospinel that is formed during the thermochemical conversion of illite contained in initial coals.[46] The presence of blocklike globules within the FS narrow fractions produced by the combustion of different types of bituminous and brown coal[3,6,25,43,44,47,48] indicates that they are formed from mineral precursors with similar compositions via a common route.

A systematic study of the composition−structure relationship of individual blocklike globules produced by the combustion of

https://doi.org/10.1021/acsomega.1c02880
ACS Omega 2021, 6, 26004−26015

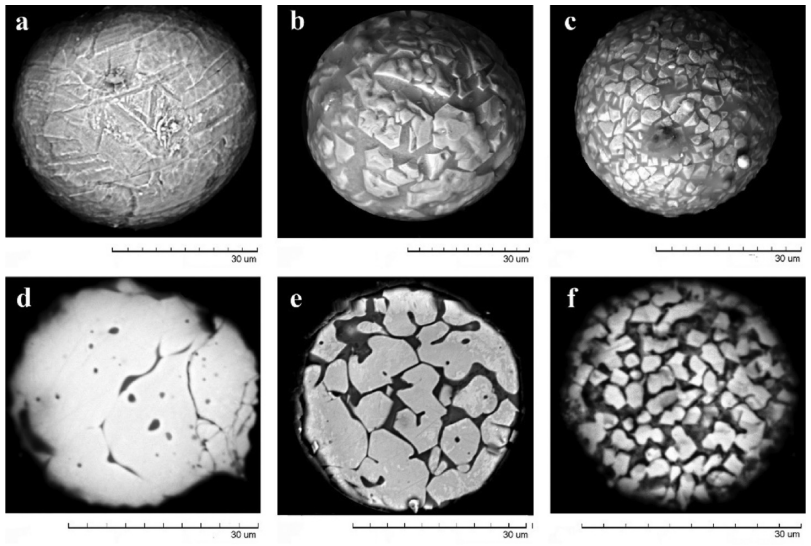

Figure 2. SEM images of the surface for different types of FSs (top row) and their polished sections (bottom row): (a, d) monoblock and (b, c, e, f) blocklike globules with a variable glass-phase content.

Table 1. Chemical Gross Composition (wt %) of Polished Sections of Blocklike Globules Produced by the Combustion of Kuznetsk Coal (Series P_2)

globule	SiO_2	Al_2O_3	FeO	CaO	MgO	Na_2O	K_2O	TiO_2	SO_3	MnO
Monoblock Globules										
9047	1.64	0.56	90.56	1.66	2.77	1.39	0.04	0.04	0.05	1.25
9046	1.90	1.05	88.90	1.60	3.76	0.94	0.04	0.02	0.00	1.71
2705	2.54	1.99	88.71	1.34	2.78	0.26	0.06	0.18	0.00	2.11
2701	5.16	3.48	83.75	2.51	2.25	0.64	0.24	0.16	0.00	1.68
5531	2.91	3.31	80.64	2.70	6.76	0.51	0.03	0.24	0.08	2.83
Blocklike Globules with a Variable Glass-Phase Content										
5518	3.92	2.70	91.42	0.24	0.41	0.44	0.00	0.07	0.00	0.78
2704	4.02	1.83	87.91	1.78	1.60	0.41	0.01	0.04	0.00	2.29
2700	7.12	2.53	85.14	1.92	1.38	0.37	0.05	0.16	0.00	1.32
2660	6.46	3.92	82.84	1.43	2.29	0.68	0.00	0.08	0.00	2.31
2934	8.89	3.84	79.98	1.45	3.30	0.70	0.04	0.29	0.00	1.50
2935	11.70	5.71	77.40	1.06	1.40	0.46	0.07	0.27	0.00	1.91
5525	6.88	6.10	76.84	3.03	1.93	0.68	0.06	0.13	0.00	4.36
8651	13.43	4.93	75.48	1.95	1.27	0.65	0.14	0.26	0.00	1.86
2698	9.73	8.46	74.51	1.03	1.24	1.73	0.35	0.19	0.00	2.61
2664	12.69	4.90	73.94	2.07	1.51	0.83	0.20	0.32	0.00	3.39
2933	12.98	6.21	72.33	1.79	3.46	0.61	0.24	0.00	0.05	2.32
8672	14.94	4.68	71.34	2.74	2.45	1.50	0.08	0.11	0.10	2.02
8650	15.77	6.90	71.47	3.54	1.28	0.76	0.08	0.18	0.00	0.00
2665	15.65	8.44	67.93	2.13	3.65	0.54	0.26	0.00	0.00	1.40
2655	14.56	7.27	67.22	3.83	4.10	1.05	0.07	0.22	0.00	1.62
2702	18.15	6.17	65.09	3.11	4.13	0.92	0.38	0.24	0.00	1.68
2699	15.74	3.51	64.77	5.98	4.60	0.38	0.06	0.07	0.00	4.75
8643	13.53	12.42	64.65	2.64	3.06	0.71	0.09	1.62	0.00	1.17
2703	15.99	10.38	64.32	2.83	5.16	0.14	0.05	0.11	0.00	0.95
8588	19.07	9.04	63.16	1.60	4.07	0.91	0.94	0.21	0.05	0.90
2659	19.90	5.31	62.00	3.06	6.75	0.66	0.11	0.17	0.03	2.01
2939	14.98	7.34	61.48	1.82	11.09	0.85	0.53	0.21	0.00	1.69
2662	18.61	12.94	55.90	1.98	8.57	0.92	0.15	0.11	0.08	0.68
5521	16.55	14.06	55.31	2.82	9.71	0.41	0.00	0.46	0.03	0.65
2658	17.81	3.31	54.46	12.04	11.12	0.90	0.12	0.09	0.00	0.14
2663	25.26	10.81	54.17	3.62	3.53	0.66	0.43	0.26	0.05	1.21
8648	22.60	7.06	54.01	6.28	6.79	0.80	0.98	0.41	0.00	0.99
8644	24.09	6.48	52.40	13.69	1.78	0.52	0.17	0.19	0.00	0.59
8646	26.07	16.35	46.01	1.88	8.13	0.6	0.15	0.6	0.05	0.1

https://doi.org/10.1021/acsomega.1c02880
ACS Omega 2021, 6, 26004−26015

Table 2. Chemical Gross Composition (wt %) of Polished Sections of Blocklike Globules Produced by the Combustion of Ekibastuz Coal (Series E)

globule	SiO_2	Al_2O_3	FeO	CaO	MgO	Na_2O	K_2O	TiO_2	SO_3	MnO
Blocklike Globules with a Variable Glass-Phase Content										
4578	10.48	5.96	76.37	1.09	3.28	1.22	0.06	0.00	0.03	1.52
4576	8.49	3.52	75.25	3.51	5.16	1.70	0.08	0.08	0.25	1.92
4581	11.06	6.55	73.98	2.65	2.64	1.07	0.01	0.20	0.24	1.52
4563	13.68	3.93	73.77	1.78	3.45	1.29	0.07	0.28	0.22	1.54
6620	15.52	3.48	73.20	1.50	3.04	1.50	0.07	0.18	0.12	1.36
4583	17.42	3.23	72.96	0.83	2.84	1.07	0.03	0.00	0.21	1.36
4565	14.22	7.39	72.36	1.84	1.15	1.41	0.16	0.13	0.22	1.09
4572	8.16	7.61	72.05	2.86	6.61	1.16	0.05	0.15	0.12	1.24
4566	13.61	7.26	71.51	1.07	3.16	1.31	0.15	0.09	0.25	1.56
5116	7.37	4.35	71.26	5.92	9.03	0.32	0.02	0.07	0.03	1.54
4569	14.04	6.13	70.94	1.12	4.96	1.09	0.03	0.10	0.12	1.45
4584	14.48	8.64	69.26	1.72	2.93	1.06	0.00	0.25	0.19	1.47
4582	15.18	8.62	69.08	1.22	2.66	1.23	0.04	0.08	0.24	1.64
6609	15.08	8.30	68.84	0.88	3.13	1.59	0.09	0.50	0.08	1.49
6663	16.86	9.24	67.96	1.15	2.06	1.32	0.18	0.17	0.05	1.00
4567	15.47	9.09	67.81	2.13	2.10	1.10	0.07	0.28	0.20	1.72
4570	16.73	7.77	67.08	2.65	2.73	1.21	0.07	0.26	0.21	1.27
4586	15.24	10.26	66.70	1.37	3.95	0.99	0.04	0.10	0.09	1.25
2694	19.81	11.09	64.32	3.72	0.51	0.27	0.06	0.10	0.00	0.00
4564	18.58	10.12	64.00	1.83	2.33	1.07	0.08	0.15	0.11	1.63
4579	21.45	9.67	62.18	1.13	3.06	0.77	0.03	0.26	0.06	1.40
4580	22.15	9.68	61.07	1.95	2.25	1.08	0.11	0.22	0.06	1.40
2668	20.08	11.35	59.56	0.75	1.08	0.37	0.00	6.05	0.05	0.51
4577	22.79	7.90	59.19	2.67	4.87	1.18	0.03	0.20	0.21	0.96
4585	19.94	10.86	59.10	2.67	4.38	1.21	0.24	0.06	0.15	1.39
6664	23.28	11.20	58.59	1.86	1.38	1.37	0.09	0.34	0.24	1.64
4574	24.94	7.50	57.73	3.19	4.42	0.99	0.11	0.16	0.03	0.92
6603	29.66	6.84	56.24	1.54	2.48	1.59	0.14	0.03	0.17	1.31
4573	31.52	4.70	55.65	1.17	4.26	1.02	0.03	0.10	0.21	1.34
6600	21.03	7.73	40.36	17.22	10.67	0.77	0.01	1.39	0.08	0.72
6599	21.81	13.36	37.74	18.80	6.29	1.13	0.05	0.26	0.05	0.50

the two main power-generating coals used in Russia was conducted to prove this hypothesis.

Composition−Structure Relationship of Blocklike FSs. An analysis of the SEM images of globules of P_2−0.05 mm series demonstrates (Figure 2a,d) that 5% of the globules consist of large sintered Al−Mg, Mn ferrospinel crystallites without a significant amount of the glass phase. These globules have a monoblock structure (Table 1), and the total content of spinel-forming components (FeO, Al_2O_3, MgO, and MnO) in them is 91−95 wt %, while the content of the main glass-forming components CaO and SiO_2 is 2.6−8.6 wt %. It should be mentioned that monoblock globules constitute 60% of all blocklike globules formed during the combustion of brown coals and contain 94−98 wt % FeO, while the total content of glass-forming oxides is 0.9−2.8 wt %.[44,47]

As the FeO content in melt droplets declines from 91 to 38 wt % and the concentration of glass-forming components increases, blocklike globules with a variable glass-phase content are formed (Figure 2b,c,e,f). The contents of SiO_2, Al_2O_3, and CaO in these globules increase within the ranges 1.6−31.5, 0.6−16.4, and 0.2−18.8 wt %, respectively (Tables 1 and 2).

The effect of the composition on the structure of FSs was studied using the dependence $SiO_2 = f(FeO)$ characterizing the iron silicate framework, dependence $SiO_2 = f(Al_2O_3)$, which allows one to identify the nature of aluminosilicate precursors involved in the formation of FSs, and dependence $CaO = f(SiO_2)$ showing the relationship between the two glass-forming components.

On the dependence $SiO_2 = f(FeO)$ (Figure 3) of the gross compositions of polished sections of individual FSs of two fractions, three groups of globules can be highlighted, whose

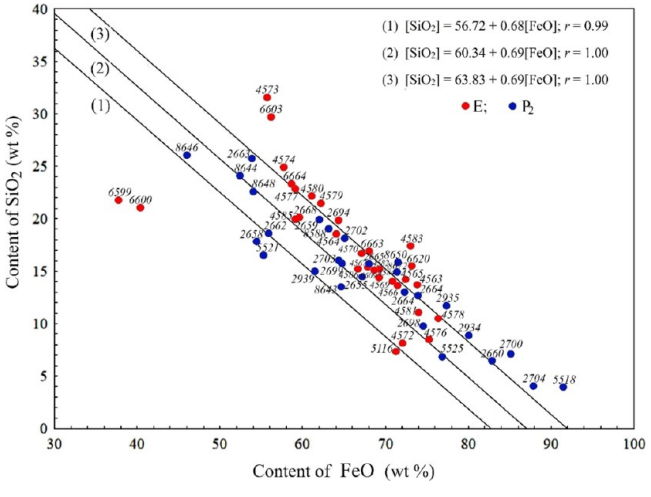

Figure 3. Dependence of the SiO_2 content on the FeO content for FSs of series P_2 and E.

https://doi.org/10.1021/acsomega.1c02880
ACS Omega 2021, 6, 26004−26015

compositions are described by linear regression equations with practically the same values of the coefficients

$$[SiO_2] = 56.72 - 0.68[FeO] \quad (1)$$

$$[SiO_2] = 60.34 - 0.69[FeO] \quad (2)$$

$$[SiO_2] = 63.83 - 0.69[FeO] \quad (3)$$

with the correlation coefficient $r = 0.99$.

Most globules belonging to the first two groups refer to the P_2−0.05 mm fraction. The third group involves more than 60% of globules of both fractions. From the above equations, it follows that the formation of the iron silicate base of FSs during the combustion of two different grades of coal involves the associates of the iron-containing precursor with quartz, in which a decrease in the FeO content and an increase in the SiO_2 concentration correspond to linear regression equations.

Figure 4 shows the dependence $SiO_2 = f(Al_2O_3)$, which allows one to determine the SiO_2/Al_2O_3 ratio of the aluminosilicate

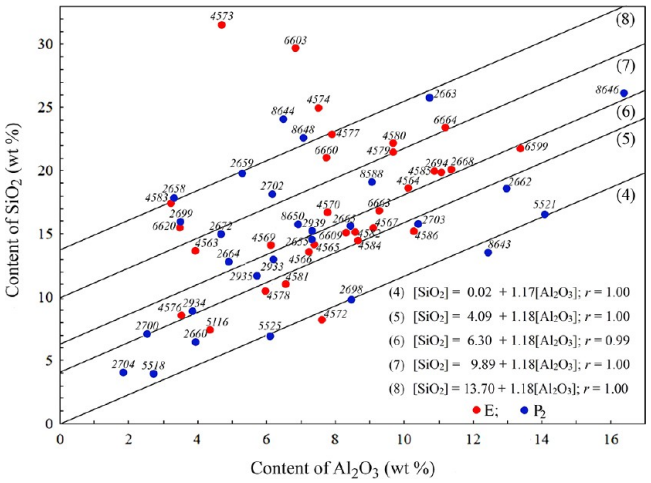

Figure 4. Dependence of the SiO_2 content on the Al_2O_3 content for FSs of series P_2 and E.

precursor involved in the formation of FSs. Five groups of globules belonging to both fractions can be identified in this dependence; their gross chemical compositions are described by the regression equations

$$[SiO_2] = 0.02 + 1.17[Al_2O_3] \quad (4)$$

$$[SiO_2] = 4.09 + 1.18[Al_2O_3] \quad (5)$$

$$[SiO_2] = 6.30 + 1.18[Al_2O_3] \quad (6)$$

$$[SiO_2] = 9.89 + 1.18[Al_2O_3] \quad (7)$$

$$[SiO_2] = 13.70 + 1.18[Al_2O_3] \quad (8)$$

with the correlation coefficient $r = 0.99$−1.00.

The coefficient in the equations shows that the globule groups are formed with the participation of an aluminosilicate precursor with a SiO_2/Al_2O_3 ratio of 1.17−1.18. The absolute term of the equation demonstrates that some additional amount of SiO_2 was included into the FS composition (being 4.1 and 6.3 wt % for groups 2 and 3, respectively). It is worth mentioning that the regression equations eqs 5 and 6 describe the composition of approximately half of the globules of both fractions. The general equations of the relationship $SiO_2 = f(Al_2O_3)$ for the analyzed FSs indicate that they are formed via similar routes and involve the same aluminosilicate precursors, which can be responsible for their structure. FSs that were not included into the main five groups are obviously formed with the involvement of the same aluminosilicate precursor and an intermediate or greater amount of SiO_2 compared to these groups.

The composition and content of the glass phase are important factors responsible for the FS structure. Four main groups of globules can be identified on the curve $CaO = f(SiO_2)$ (Figure 5), which shows the pattern of the relationship between the two

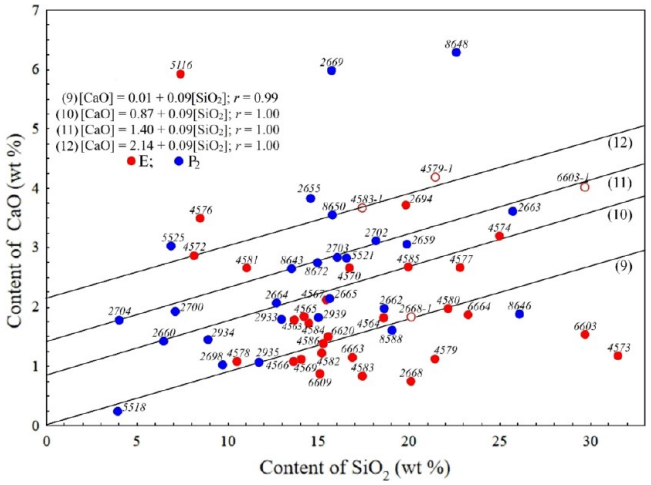

Figure 5. Dependence of the CaO content on the SiO_2 content for FSs of series P_2 and E.

glass-forming components; the gross chemical compositions of these groups correspond to the regression equations

$$[CaO] = 0.01 + 0.09[SiO_2] \quad (9)$$

$$[CaO] = 0.87 + 0.09[SiO_2] \quad (10)$$

$$[CaO] = 1.40 + 0.09[SiO_2] \quad (11)$$

$$[CaO] = 2.14 + 0.09[SiO_2] \quad (12)$$

with the correlation coefficient $r = 0.99$−1.0.

Most globules under study (75%) are described by the aforelisted regression equations; the coefficients are identical (0.09), and the absolute term of the equation increases within the range 0.01−2.14. Importantly, the globules of series P_2 are characterized by a higher CaO content than that in the E−0.05 mm fraction of FSs. Approximately 25% of globules of the E−0.05 mm fraction are characterized by a high SiO_2 content (15−32 wt %) and a low CaO content (<2 wt %) and are not described by the four aforelisted regression equations $CaO = f(SiO_2)$. Taking into account the MgO concentration, the composition of these globules corresponds to one of the aforelisted regression coefficients $CaO = f(SiO_2)$ (Figure 5). In particular, the gross chemical composition of globule E2668 corresponds to eq 9; the gross chemical composition of globule E6603 corresponds to eq 11, and those of globules E4583 and E4579 correspond to eq 12 (Figure 5). This correlation implies that magnesium oxide can act as a glass-forming component along with CaO. Globules $P_2$8644, $P_2$2658, E6600, and E6599 with CaO contents of 12−18.8 wt % form a separate group. MgO concentrations above 10 wt % are observed in FSs $P_2$2939, $P_2$2658, and E6600.

https://doi.org/10.1021/acsomega.1c02880
ACS Omega 2021, 6, 26004−26015

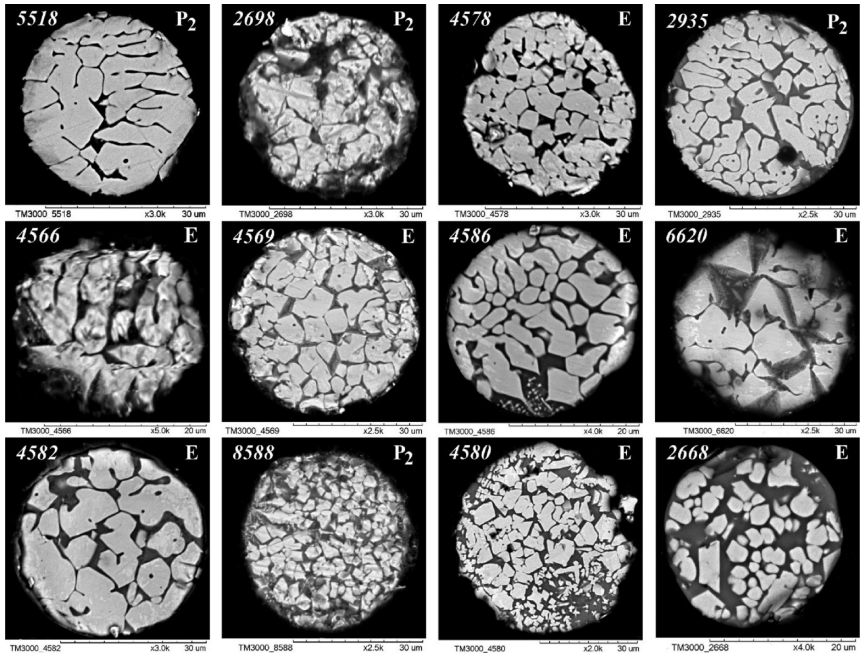

Figure 6. SEM images of FS polished sections of series P_2 and E corresponding to the equation $[CaO] = 0.01 + 0.09[SiO_2]$ (Figure 5).

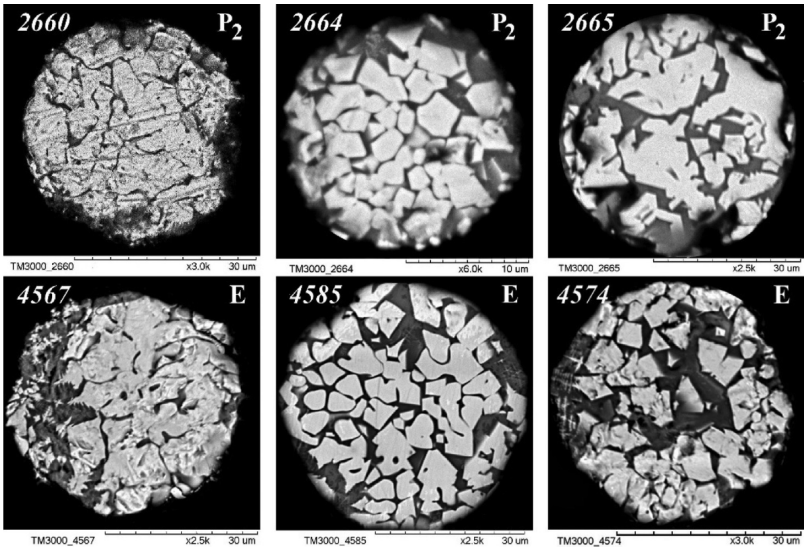

Figure 7. SEM images of FS polished sections of series P_2 and E corresponding to the equation $[CaO] = 0.87 + 0.09[SiO_2]$ (Figure 5).

Figures 6−10 show the SEM images of the polished sections of globules characterizing the change in their structure with an increase in the concentration of SiO_2 and a decrease in the content of spinel-forming oxides (FeO, Al_2O_3, and MgO) for the FS groups presented in Figure 5. The SEM images of the first (Figure 6), second, and fourth (Figures 7 and 9) groups show globules of both fractions with the FeO content lying in the ranges 91.4−59.6, 82.8−57.7, and 72−62.5 wt %, respectively. The third group (Figure 8) contains only globules of the P_2−0.05 mm fraction with an FeO content of 87.9−54.2 wt %. The number of the globule is shown in the left corner of all the SEM images; information in the right corner denotes whether the globule belongs to the fraction of P_2 or E series.

Along with the groups listed above, each fraction contains two globules with CaO concentrations of 12−18.8 wt % and a high content of the glass phase (Tables 1 and 2). The SEM images of these globules are shown in Figure 10 in the descending order of FeO concentration in the range of 54.5−37.7 wt %.

The general equations representing the relationship between the compositions of major components of individual FSs produced by the combustion of two types of coal demonstrate that their precursors were of the same nature. Meanwhile, the broad variation of the composition of individual globules of the same size indicates that there is significant heterogeneity of distribution of mineral components within coal. An analysis of the relationship between the major component composition and structure of the polished sections of individual globules belonging to the five groups listed above (Figures 6−10) demonstrated that the globules were formed from ferrospinel crystallites of different shapes and sizes. There is a general trend toward increasing glass-phase content and declining size of ferrospinel crystallites as FeO concentration decreases.

https://doi.org/10.1021/acsomega.1c02880
ACS Omega 2021, 6, 26004−26015

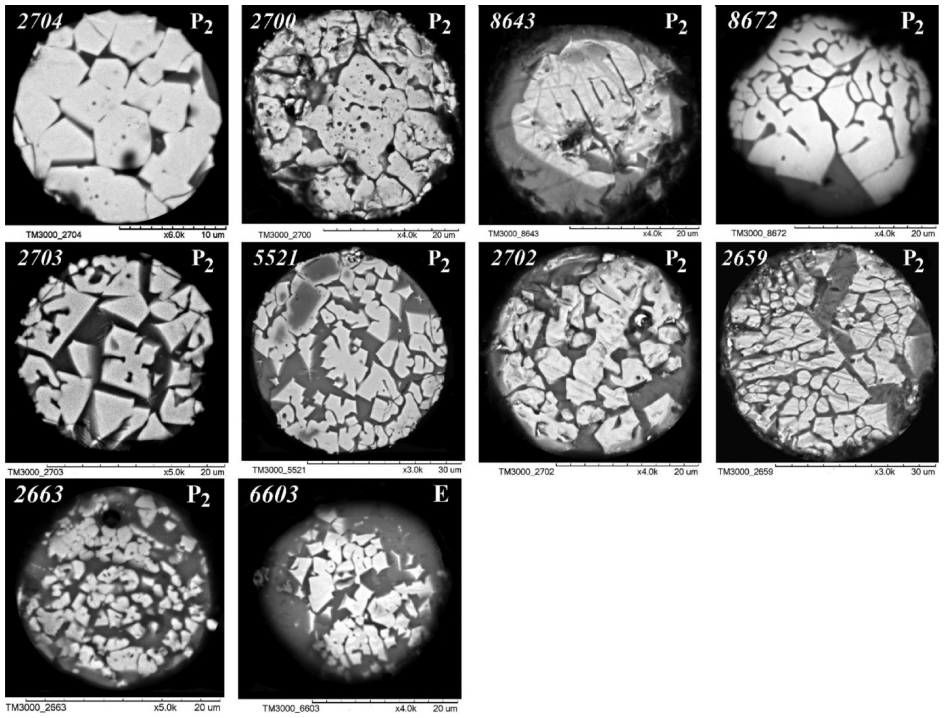

Figure 8. SEM images of FS polished sections of series P_2 and E corresponding to the equation $[CaO] = 1.40 + 0.09[SiO_2]$ (Figure 5).

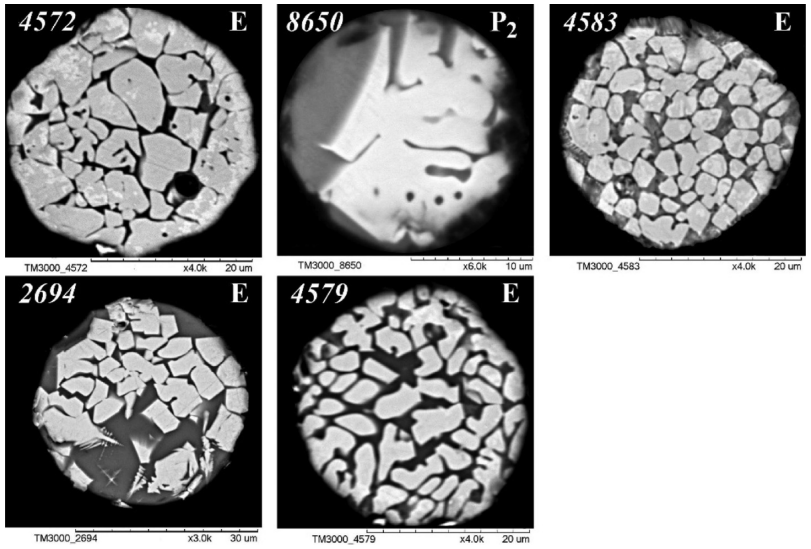

Figure 9. SEM images of FS polished sections of series P_2 and E corresponding to the equation $[CaO] = 2.14 + 0.09[SiO_2]$ (Figure 5).

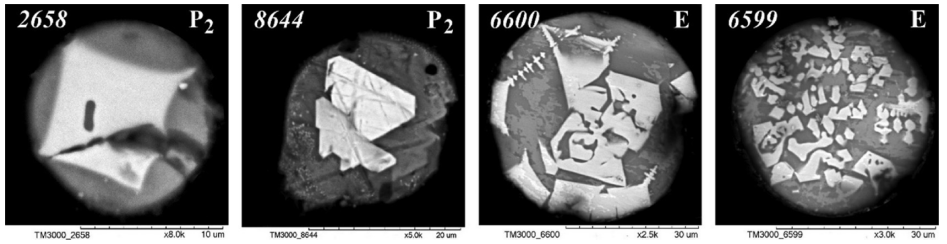

Figure 10. SEM images of FS polished sections of series P_2 and E with a CaO content of 12−19 wt %.

Routes of Formation of Blocklike FSs. In order to identify the routes of formation of FSs, one needs to discuss the features of thermochemical conversion of iron-containing and aluminosilicate mineral precursors of the initial coals.

Coals deposited in the Ekibastuz Basin have thin alternating layers of the organic and mineral matter. This structure of the coal deposit results in a high content of mineral substances A^d = 45 wt %, which are separated during coal beneficiation only to a

https://doi.org/10.1021/acsomega.1c02880
ACS Omega 2021, 6, 26004−26015

small extent. The coals are characterized by low contents of phosphorus (0.07−0.12%) and sulfur (0.2−0.4%).[49] Most of the mineral matter is represented by clay minerals (54%), quartz (28%), siderite (10%), calcite (5%), magnetite (2%), and gypsum (2%). The content of plagioclases in different strata may vary from 10.1 to 18.7% for albite and from 0 to 24.5% for anorthite. Quartz is present in the coals in two forms: terrigenous (grains of varying roundness) and syngenetic ones (fine aggregates and veins).[50,51] Siderite, the predominant iron-containing mineral form, occurs as small lenses and spherulites. Pyrite is present as a fine-grained impurity or occurs in its mixture with calcite, which can replace kaolinite in unit cell cavities.[3,49,50]

Coals mined from the Kuznetsk Basin are characterized by a low sulfur content of <1%; the ash content in them is 10−15%. The phase composition of the mineral matter in coal is represented by clay minerals (54%), quartz (14%), siderite (10.5%), gypsum (7.5%), plagioclases (7.5%), and calcite (2%).[50] Together with quartz, clay minerals (hydromica and kaolinite) constitute the main portion of the mineral matter. Quartz is separated into its unbound ("free") form and quartz bound to argillaceous particles (grains sized 0.03−1 mm).[51] Siderite is present as spherulite structures sized <0.5 mm. Pyrite impurity is distributed over the organic matter of coal as disseminated grains, single crystals sized 0.001−0.5 mm, and spherical structures 0.02−2 mm in diameter.[3,49]

The thermochemical transformation of the mineral precursors of both coals leads to the formation of blocklike globules, whose major component composition corresponds to the general equations of the relationship. The nature of the iron-containing precursor is reflected in the composition of ferrospinel crystallites and the globule structure.

The monoblock globules of the P_2−0.05 mm fraction are formed by large sintered ferrospinel crystallites with an FeO content of 80.6−90.6 wt % and MgO and MnO contents of up to 6.8 and 2.8 wt %, respectively (Table 1 and Figure 2a, d). The high contents of MgO and MnO in the globules demonstrate that these oxides were formed from siderite containing isomorphic impurities of magnesium and manganese carbonates. The decomposition of the mixture of carbonates, including calcite, is accompanied by the formation of a low-temperature eutectic corresponding to the calcio-wüstite phase, followed by its oxidation to ferrospinel and hematite.[3,52]

Along with monoblock globules, the P_2−0.05 mm fraction contains FSs having a variable content of the glass phase and a high FeO content (91−77 wt %) (Table 1 and Figure 2b,c,e,f). The E−0.05 mm fraction does not contain globules of this type, while the content of FeO in blocklike globules is ≤76 wt %. The associations of siderite (pyrite) and calcite, aluminosilicate minerals, and quartz with varied contents of the components observed for different coal types play a crucial role in the FS formation having a variable glass-phase content. These associations significantly facilitate the coalescence of the spatially localized products of thermochemical conversion of mineral components.[52−54]

In the initial coals mined from the Kuznetsk and Ekibastuz deposits, the silicate component contains plagioclases (feldspars) (7.5 and 24.5%, respectively) along with quartz, kaolinite, and hydromica.[49,51] Among the silicate forms listed above, the SiO_2/Al_2O_3 ratio is 1.18 only for the extreme member in the series of Na−Ca feldspars (anorthite: $CaAl_2Si_2O_8$),[55] which coincides with the coefficient values 1.17−1.18 in the equations $SiO_2 = f(Al_2O_3)$ characterizing the aluminosilicate composition of the five FS groups (Figure 4). Coalescence in the carbon matrix of the spatially localized products of thermochemical conversion of siderite associated with quartz, calcite, and anorthite gives rise to microdroplets of the melt. The formation of melt microdrops in the $FeO−SiO_2−Al_2O_3−CaO$ system occurs with the participation of the same low-temperature eutectics on the base of the reduced Fe^{2+} forms.[25,43,47,56]

For the vast majority of the studied FSs, the CaO concentration does not exceed 5 wt %, and the total content of FeO, SiO_2, and Al_2O_3 is 84−98 wt % (Tables 1 and 2). Therefore, the analysis of the formation and phase transformations of melt microdrops in a reducing medium can be carried out using the $FeO−SiO_2−Al_2O_3$ ternary phase diagram.[57] The composition of the melt of the individual blocklike FSs corresponds to the compositions of the phase boundaries between the primary crystallization fields of wüstite, fayalite, and hercynite (Figure 11). In the same area, the compositions of the FS narrow fractions and their concentrates formed during the combustion of different types of coals are localized.[58] Anorthite is the main aluminosilicate precursor involved in the FS formation (Figures 11 and 4). The high quartz content in the Ekibastuz coal leads to the formation of FSs with a higher SiO_2 content, which explains the deviation from the trend corresponding to anorthite. Crystallization of the melt and oxidation of Fe^{2+} to Fe^{3+} lead to the decomposition of ternary and binary compounds, including fayalite (Fe_2SiO_4), and the formation of magnetite or solid solutions based on magnetite (or on hematite in air) and silica.

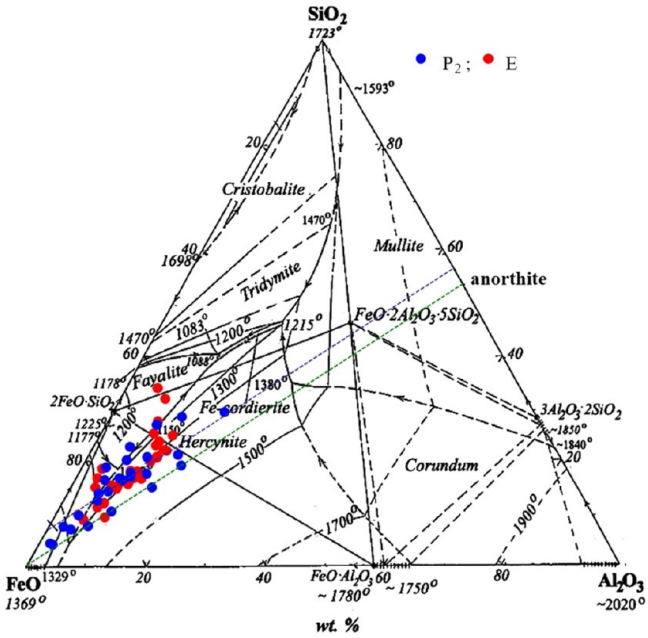

Figure 11. Compositions of individual investigated FSs.

To determine the range of changes in the composition of the solid solution, the compositions of the local points of the crystallites of the ferrospinel in globules were studied, whose composition is described by eq 3 (Figure 5 and Table 3). Table 3 lists the compositions of local points (4 μm in diameter) of ferrospinel crystallites with the SiO_2 content of <3 wt %. It follows from the reported data that as FeO concentration in the local points (92−22.6 wt %) decreases, the content of other spinel-forming oxides capable of isomorphic substitution of iron increases: Al_2O_3, (2.2−55.5 wt %); MgO, (0.6−18.9 wt %); and

https://doi.org/10.1021/acsomega.1c02880
ACS Omega 2021, 6, 26004−26015

Table 3. Chemical Composition in Local Points (wt %) of the Ferrospinel Crystallites of Blocklike FSs (P_2 and E Series) in Groups with Different Contents of CaO

globule	Al_2O_3	FeO	CaO	MgO	TiO_2	MnO
			Group (3) $[CaO] = 1.40 + 0.09[SiO_2]$			
$P_2$2704	2.2−3.2	88.2−89.4	0.3−1.2	1.2−1.7	0−0.1	2.0−2.7
$P_2$8643	2.6−3.4	87.4−89.1	0.6−1.0	3.0−4.1	0−0.2	1.3−1.7
$P_2$8672	2.7−4.1	88.5−89.2	0−0.3	2.6−3.3	0.1−0.7	1.1−2.5
$P_2$2703	7.0−10.1	77.1−84.5	0.1−0.6	4.3−7.1	0−0.6	0.2−1.7
$P_2$5521	7.3−12.8	70.6−83.9	0−0.7	6.2−10.6	0−1.1	0.5−1.8
$P_2$5521[a]	55.4−55.5	22.6−24.0	0.1−0.3	17.8−18.9	0.3	0.4−0.5
$P_2$2702	3.2−5.2	79.2−87.1	0−1.7	4.6−6.5	0−0.5	1.5−4.5
$P_2$2663	5.1−8.3	77.0−84.6	1.2−1.8	5.2−7.3	0−0.9	0.8−1.6
			Group (5) CaO = 12 − 18.8 wt %			
$P_2$2658	1.3−2.6	71.9−85.5	0.2−1.6	10.8−17.8	0−0.5	0.1−0.7
$P_2$8644	1.8−3.2	89.1−91.7	0.1−1.2	2.2−3.0	0.1−0.8	0.2−1.3
E6600	11.0−12.9	69.3−70.8	0.1−1.1	11.3−15.7	0−0.2	0.2−1.0
E6599	13.9−16.3	64.6−70.7	0.2−1.1	12.7−14.4	0−0.4	0.3−0.8

[a]Dark areas.

MnO, (0.4−2.7 wt %). The dark local points of globule $P_2$5521 are characterized by the lowest FeO content (22.6−24.0 wt %) and the highest contents of Al_2O_3 and MgO (55.4−55.5 and 17.8−18.9 wt %, respectively) (Figure 8).

The broad variation of the composition of local points of ferrospinel crystallites is also typical of globules $P_2$2658, $P_2$8644, E6600, and E6599 with a CaO content of 12.04−18.8 wt % (Table 3). The dark areas within crystallites with high Al_2O_3 and MgO contents are also observed for these globules (Figure 10 and Table 3). It is clear that high MgO concentrations in the composition of the individual globules and ferrospinels are indicative of the high content of dolomite ($MgCO_3$) within the precursors involved in formation of these globules.

A widely varying composition of local points of ferrospinel crystallites indicates in favor of their formation not from a homogeneous melt but due to the sintering of individual fragments in the porous carbon matrix. Crystallization of magnetite-based Al, Mg ferrospinel occurs when the concentration of spinel-forming oxides in local areas exceeds 85 wt %,[13] which corresponds to the magnetite crystallization region in the $FeO−Fe_2O_3−SiO_2$ system in an oxygen atmosphere.[59] The size and shape of these local areas characterize the broad variation of the size of crystallites within individual globules (Figures 6−10).

A similar route for the formation of blocklike FSs with the participation of anorthite as an aluminosilicate precursor and a wide variation in the composition of local points of the ferrospinel crystals was determined for FSs obtained by burning brown and bituminous coals.[44,47] In particular, three groups of FSs were identified on the dependence $SiO_2 = f(Al_2O_3)$ for these globules; their compositions were described by linear regression coefficients with coefficients 1.17−1.19 and the absolute terms equal to 0.4, 7.82, and 14.33. Three groups of globules whose compositions are described by the general regression equations with coefficients 0.09 and the absolute terms 0.17, 1.0, and 2.05 were differentiated on the dependence $CaO = f(SiO_2)$. The group of globules whose composition corresponds to the equation $[CaO] = 0.17 + 0.09[SiO_2]$ contains globule S2790, for which the dark local areas of large blocks contain 32−47 wt % Al_2O_3 and 62−48 wt % FeO. Similar dark local areas with high contents of Al_2O_3 and MgO are also seen in other globules (e.g., B1268 and B6221).[44,47]

Thus, an analysis of our results and the literature data[43,44,47] infers that anorthite in the initial brown and hard coals acts as an aluminosilicate precursor in the FS formation with a blocklike structure. Magnetite-based ferrospinel crystallizes from the melts with different compositions when the concentration of spinel-forming oxides in the local areas becomes ≥85 wt %.[13]

As concentrations of FeO and SiO_2 within individual FSs are varied in the ranges 91.4−37.2 and 3.9−31.5 wt %, respectively, the glass-phase content increases monotonically in all the groups (Figures 6−9). If it is assumed that melt droplets stay in an oxidizing atmosphere for the same time, then with a decrease in the concentration of iron, the degree of its oxidation increases. In this case, the increase in the glass-phase content in FSs can be attributed to the fact that the liquation zone in the $FeO−Fe_2O_3−SiO_2$ system becomes larger with increasing oxidative potential.[59] This process is additionally affected by the increasing concentration of CaO within the globules. Thus, the high CaO concentration (12−18.8 wt %) in globules $P_2$2658, $P_2$8644, E6600, and E6599 (Figure 10) has a significant effect on the increase in the glass-phase content. A similar effect of the high CaO concentration (18−25 wt %) on the glass-phase content was demonstrated for the FSs formed during the combustion of brown coal.[44,47] The content of the glass phase also tends to increase for calcium-rich industrial slags, which is attributed to the increasing content of ferrite complexes $[Fe^{3+}O_2]^-$ and $[Fe^{3+}{}_2O_5]^{4-}$ in the melt.[60,61]

Along with the high content of the glass phase, globules $P_2$2658, $P_2$8644, and E6600 (Figure 10) include one or more large ferrospinel crystallites. This is due to the participation of excluded siderite particles, whose fragmentation contributes to the formation of large-block FSs.[3] During coal combustion, the included dispersed siderite particles can coalesce with other melt microdroplets, thus giving rise to fine-grained crystallites within FSs.

CONCLUSIONS

As a result of the performed study, the content of different morphological types of individual FSs of fractions −0.05 mm isolated from fly ash produced by the burning of coals from the Kuznetsk and Ekibastuz Basins was determined. The contents of blocklike FSs are 19 and 11%, of skeletal−dendritic FSs are 50 and 64%, of spongy FSs are 5 and 8%, and of plerospheres are 7 and 4%, respectively. The relationship between the composition and structure of individual blocklike FSs of these fractions was studied by the SEM−EDS (energy-dispersive spectroscopy)

https://doi.org/10.1021/acsomega.1c02880
ACS Omega 2021, 6, 26004−26015

method. The common groups of globules have been distinguished, whose gross chemical compositions of polished sections are fitted by the equations describing the relationship between concentrations $SiO_2 = f(FeO)$; $SiO_2 = f(Al_2O_3)$; and $CaO = f(SiO_2)$. The common routes of formation of FSs have been identified; they included the stages of sequential conversion of the dispersed products of thermochemical conversion of the associates of mineral precursors in the porous carbon matrix. The monoblock globules were shown to consist of large sintered crystallites of Mg, Mn ferrospinel, which are formed from the excluded siderite particles containing isomorphic inclusions of magnesium and manganese carbonates. Blocklike FSs of both fractions with a variable content of the glass phase are formed during thermochemical conversion of the associates of siderite, quartz, calcite, and anorthite with the SiO_2/Al_2O_3 ratio of 1.18, which corresponds to the coefficients in the general relationship equations $SiO_2 = f(Al_2O_3)$.

Four main groups of FSs can be differentiated from the relationship $CaO = f(SiO_2)$, which include globules of both fractions whose composition is fitted by linear regression equations. An analysis of the SEM images of the polished sections of globules belonging to these groups demonstrates that the size of ferrospinel crystallites decreases gradually with the increasing concentration of the glass-forming components. The crystallite size and shape were shown to depend on the size of the local melt region where the concentration of spinel-forming oxides is >85 wt %. The increase in the content of the glass phase in globules with a high CaO content (12−18.8 wt %) is attributed to the fact that concentrations of $[Fe^{3+}O_2]^-$ and $[Fe^{3+}{}_2O_5]^{4-}$ ferrite complexes additionally increase as the oxidative potential of calcium-rich melts increases.

EXPERIMENTAL SECTION

The FS narrow fractions sized −0.05 mm isolated from fly ashes produced by the combustion of pulverized hard coals of grade SS (mvb) from the the Ekibastuz Basin (series E) and grade T (sa) from the Kuznetsk Basin (series P2) were used as study objects. Combustion was performed in BKZ-420-140 and BKZ-320-140 boiler furnaces (flame core temperature, 1700 °C) with a dry ash removal unit at the Omsk Thermal Power Station-4. Fly ash was sampled from fields 1 and 2 of an electrostatic precipitator. The FS narrow fractions were obtained my multistage isolation from MCs involving particle size classification, followed by hydrodynamic separation to remove nonmagnetic impurities. Detailed information about the methods used for isolating fractions E−0.05 mm (Fe_2O_3 content, 71.32 wt %) and P_2−0.05 mm (Fe_2O_3 content, 66.38 wt %) and determining the chemical and phase compositions was reported in ref 33.

In order to investigate the structure and composition of individual globules, we used polished sections of FSs produced by fixing FSs in epoxy resin, followed by grinding, polishing, and deposing a ∼20 nm thick platinum layer. The polished sections of individual FSs were analyzed using a TM-3000 scanning electron microscope (Hitachi) coupled with an energy-dispersive X-ray spectrometer with a Flash 430 H detector at an accelerating voltage of 15 kV in the mapping mode. The quality of the spectrum assembly determined the data accumulation time, which exceeded 10 min. This made it possible to quantify the composition of individual globules. The gross chemical composition of the entire cross-section surface and the compositions of local points with a diameter of 4 μm were determined. All the elements were calculated as appropriate oxides, and iron was calculated as FeO.[44]

AUTHOR INFORMATION

Corresponding Author

Alexander G. Anshits − *Institute of Chemistry and Chemical Technology SB RAS, Federal Research Center "Krasnoyarsk Science Center SB RAS", Krasnoyarsk 660036, Russia; Siberian Federal University, Krasnoyarsk 660041, Russia;* orcid.org/0000-0002-5259-0319; Email: anshits@icct.ru

Authors

Natalia N. Anshits − *Institute of Chemistry and Chemical Technology SB RAS, Federal Research Center "Krasnoyarsk Science Center SB RAS", Krasnoyarsk 660036, Russia*

Elena V. Fomenko − *Institute of Chemistry and Chemical Technology SB RAS, Federal Research Center "Krasnoyarsk Science Center SB RAS", Krasnoyarsk 660036, Russia;* orcid.org/0000-0003-0929-807X

Complete contact information is available at: https://pubs.acs.org/10.1021/acsomega.1c02880

Notes

The authors declare no competing financial interest.

ACKNOWLEDGMENTS

This work was conducted within the framework of the budget project # 121031500198-3 for the Institute of Chemistry and Chemical Technology SB RAS using for SEM−EDS study the equipment of the Krasnoyarsk Regional Research Equipment Centre of SB RAS. The authors would like to thank A. M Zhizhaev for SEM−EDS analysis of FS polished sections and M. A. Fedorchak for help in the quantitative processing of SEM−EDS spectra.

REFERENCES

(1) Clarke, L. B.; Sloss, L. L. *Trace Elements-Emissions from Coal Combustion and Gasification. IEACR/49*; IEA Coal Research: London, 1992 https://www.sustainable-carbon.org/report/trace-elements-emissions-from-coal-combustion-and-gasification-ieacr-49/.

(2) Cloke, M.; Lester, E. Characterization of coals for combustion using petrographic analysis: a review. *Fuel* **1994**, *73*, 315−320.

(3) Kizil'shtein, L. Ya.; Dubov, I. V.; Shpitsgluz, A. L.; Parada, S. G. *Komponenty zol i shlakov TES (Components of Ash and Slag of TPSs)*; Energoatomizdat: Moscow, 1995. (In Russian).

(4) Hower, J. C.; Maroto-Valer, M. M.; Taulbee, D. N.; Sakulpitakphon, T. Mercury Capture by Distinct Fly Ash Carbon Forms. *Energy Fuels* **2000**, *14*, 224−226.

(5) Goodarzi, F. Assessment of elemental content of milled coal, combustion residues, and stack emitted materials: Possible environmental effects for a Canadian pulverized coal-fired power plant. *Int. J. Coal Geol.* **2006**, *65*, 17−25.

(6) Vassilev, S. V.; Menendez, R.; Borrego, A. G.; Diaz-Somoano, M.; Rosa Martinez-Tarazona, M. Phase-mineral and chemical composition of coal fly ashes as a basis for their multicomponent utilization. 3. Characterization of magnetic and char concentrates. *Fuel* **2004**, *83*, 1563−1583.

(7) Sharonova, O. M.; Anshits, N. N.; Yumashev, V. V.; Anshits, A. G. Composition and morphology of char particles of fly ashes from industrial burning of high-ash coals with different reactivity. *Fuel* **2008**, *87*, 1989−1997.

(8) Fomenko, E. V.; Anshits, N. N.; Vasilieva, N. G.; Mikhaylova, O. A.; Rogovenko, E. S.; Zhizhaev, A. M.; Anshits, A. G. Characterization of Fly Ash Cenospheres Produced from the Combustion of Ekibastuz Coal. *Energy Fuels* **2015**, *29*, 5390−5403.

(9) Yan, L.; Gupta, R. P.; Wall, T. F. The implication of mineral coalescence behaviour on ash formation and ash deposition during pulverised coal combustion. *Fuel* **2001**, *80*, 1333−1340.

(10) Xu, M.; Yu, D.; Yao, H.; Liu, X.; Qiao, Y. Coal combustion-generated aerosols: Formation and properties. *Proc. Combust. Inst.* **2011**, *33*, 1681−1697.
(11) Buhre, B.; Hinkley, J.; Gupta, R.; Nelson, P.; Wall, T. Fine ash formation during combustion of pulverised coal−coal property impacts. *Fuel* **2006**, *85*, 185−193.
(12) Helble, J. J.; Sarofim, A. F. Influence of char fragmentation on ash particle size distributions. *Combust. Flame* **1989**, *76*, 183−196.
(13) Srinivasachar, S.; Helble, J. J.; Boni, A. A. Mineral behavior during coal combustion 1. Pyrite transformations. *Prog. Energy Combust. Sci.* **1990**, *16*, 281−292.
(14) Yan, L.; Gupta, R.; Wall, T. Fragmentation Behavior of Pyrite and Calcite during High-Temperature Processing and Mathematical Simulation. *Energy Fuels* **2001**, *15*, 389−394.
(15) Wen, C.; Gao, X.; Yu, Y.; Wu, J.; Xu, M.; Wu, H. Emission of inorganic PM_{10} from included mineral matter during the combustion of pulverized coals of various ranks. *Fuel* **2015**, *140*, 526−530.
(16) Zhang, L.; Ninomiya, Y. Emission of suspended PM_{10} from laboratory-scale coal combustion and its correlation with coal mineral properties. *Fuel* **2006**, *85*, 194−203.
(17) Blissett, R. S.; Rowson, N. A. A review of the multi-component utilization of coal fly ash. *Fuel* **2012**, *97*, 1−23.
(18) Yao, Z. T.; Ji, X. S.; Sarker, P. K.; Tang, J. H.; Ge, L. Q.; Xia, M. S.; Xi, Y. Q. A comprehensive review on the applications of coal fly ash. *Earth-Sci. Rev.* **2015**, *141*, 105−121.
(19) Belviso, C. State-of-the-art applications of fly ash from coal and biomass: A focus on zeolite synthesis processes and issues. *Prog. Energy Combust. Sci.* **2018**, *65*, 109−135.
(20) Ahmaruzzaman, M. A review of the utilization of fly ash. *Prog. Energy Combust. Sci.* **2010**, *36*, 327−363.
(21) Iyer, R. S.; Scott, J. A. Power station fly ash − a review of valueadded utilization outside of the construction industry. *Resour., Conserv. Recycl.* **2001**, *31*, 217−228.
(22) Querol, X.; Moreno, N.; Umaña, J. C.; Alastuey, A.; Hernández, E.; López-Soler, A.; Plana, F. Synthesis of zeolites from coal fly ash: An overview. *Int. J. Coal Geol.* **2002**, *50*, 413−423.
(23) Ahmaruzzaman, M.; Gupta, V. K. Application of Coal Fly Ash in Air Quality Management. *Ind. Eng. Chem. Res.* **2012**, *51*, 15299.
(24) Ge, J.; Yoon, S.; Choi, N. Application of fly ash as an adsorbent for removal of air and water pollutants. *Appl. Sci.* **2018**, *8*, 1116.
(25) Sokol, E. V.; Kalugin, V. M.; Nigmatulina, E. N.; Volkova, N. I.; Frenkel, A. E.; Maksimova, N. V. Ferrospheres from fly ashes of Chelyabinsk coals: chemical composition, morphology and formation conditions. *Fuel* **2002**, *81*, 867−876.
(26) Zhao, Y.; Zhang, J.; Sun, J.; Bai, X.; Zheng, C. Mineralogy, Chemical Composition, and Microstructure of Ferrospheres in Fly Ashes from Coal Combustion. *Energy Fuels* **2006**, *20*, 1490−1497.
(27) Hower, J. C.; Rathbone, R. F.; Robertson, J. D.; Peterson, G.; Trimble, A. S. Petrology, mineralogy, and chemistry of magnetically-separated sized fly ash. *Fuel* **1999**, *78*, 197−203.
(28) Hulett, L. D., Jr.; Weinberger, A. J.; Northcutt, K. J.; Ferguson, M. Chemical Species in Fly Ash from Coal-Burning Power Plants. *Science* **1980**, *210*, 1356−1358.
(29) Ramsden, A. R.; Shibaoka, M. Characterization and analysis of individual fly-ash particles from coal fired power stations by a combination of optical microscopy, electron microscopy and quantitative electron microprobe analysis. *Atmos. Environ.* **1982**, *16*, 2191−2206.
(30) Panteleev, V.; Larina, E.; Melentev, V.; Sergeeva, T.; Mokrushin, A. *Composition and properties of fly ashes and slags from TPS*; Energoatomizdat: Handbook, Leningrad, 1985. (In Russian).
(31) Querol, X.; Fernández-Turiel, J.; López-Soler, A. Trace elements in coal and their behaviour during combustion in a large power station. *Fuel* **1995**, *74*, 331−343.
(32) Vassilev, S. V.; Vassileva, C. G. Mineralogy of combustion wastes from coal-fired power stations. *Fuel Process. Technol.* **1996**, *47*, 261−280.
(33) Sharonova, O. M.; Anshits, N. N.; Solovyov, L. A.; Salanov, A. N.; Anshits, A. G. Relationship between composition and structure of globules in narrow fractions of ferrospheres. *Fuel* **2013**, *111*, 332−343.
(34) Bayukov, O. A.; Anshits, N. N.; Balaev, A. D.; Sharonova, O. M.; Rabchevskii, E. V.; Petrov, M. I.; Anshits, A. G. Mossbauer study of magnetic microspheres isolated from power plant fly ash. *Inorg. Mater.* **2005**, *41*, 50−59.
(35) Bajukov, O. A.; Anshits, N. N.; Petrov, M. I.; Balaev, A. D.; Anshits, A. G. Composition of ferrospinel phase and magnetic properties of microspheres and cenospheres from fly ashes. *Mater. Chem. Phys.* **2009**, *114*, 495−503.
(36) Anshits, A. G.; Kondratenko, E. V.; Fomenko, E. V.; Kovalev, A. M.; Bajukov, O. A.; Anshits, N. N.; Sokol, E. V.; Kochubey, D. I.; Boronin, A. I.; Salanov, A. N.; Koshcheev, S. V. Physicochemical and catalytic properties of glass crystal catalysts for the oxidation of methane. *J. Mol. Catal. A: Chem.* **2000**, *158*, 209−214.
(37) Vereshchagin, S. N.; Kondratenko, E. V.; Rabchevskii, E. V.; Anshits, N. N.; Solov'ev, L. A.; Anshits, A. G. New approach to the preparation of catalysts for the oxidative coupling of methane. *Kinet. Catal.* **2012**, *53*, 449−455.
(38) Anshits, A. G.; Bayukov, O. A.; Kondratenko, E. V.; Anshits, N. N.; Pletnev, O. N.; Rabchevskii, E. V.; Solovyov, L. A. Catalytic properties and nature of active centers of ferrospheres in oxidative coupling of methane. *Appl. Catal., A* **2016**, *524*, 192−199.
(39) Kirik, N. P.; Anshits, N. N.; Rabchevskii, E. V.; Solov'ev, L. A.; Anshits, A. G. Effect of HF modification on the catalytic properties of ferrospheres in the oxidative coupling of methane. *Kinet. Catal.* **2019**, *60*, 196−204.
(40) Kopytov, M. A.; Golovko, A. K.; Kirik, N. P.; Anshits, A. G. Thermal transformations of highmolecular-mass-components of heavy petroleum residues. *Pet. Chem.* **2013**, *53*, 14−19.
(41) Golovko, A. K.; Kopytov, M. A.; Sharonova, O. M.; Kirik, N. P.; Anshits, A. G. Cracking of heavy oils using catalytic additives based on coal fly ash ferrospheres. *Catal. Ind.* **2015**, *7*, 293−300.
(42) Vereshchagina, T. A.; Fedorchak, M. A.; Sharonova, O. M.; Fomenko, E. V.; Shishkina, N. N.; Zhizhaev, A. M.; Kudryavtsev, A. N.; Frank, L. A.; Anshits, A. G. $Ni2^{+-}$zeolite/ferrosphere and Ni−silica/ferrosphere beads for magnetic affinity separation of histidine-tagged proteins. *Dalton Trans.* **2016**, *45*, 1582−1592.
(43) Sharonova, O. M.; Anshits, N. N.; Fedorchak, M. A.; Zhizhaev, A. M.; Anshits, A. G. Characterization of Ferrospheres Recovered from High-Calcium Fly Ash. *Energy Fuels* **2015**, *29*, 5404−5414.
(44) Anshits, N. N.; Fedorchak, M. A.; Fomenko, E. V.; Mazurova, E. V.; Anshits, A. G. Composition, Structure, and Formation Routes of Blocklike Ferrospheres Separated from Coal and Lignite Fly Ashes. *Energy Fuels* **2020**, *34*, 3743−3754.
(45) Anshits, N. N.; Fedorchak, M. A.; Sharonova, O. M.; Kirik, N. P.; Shishkina, N. N.; Zhizhaev, A. M.; Anshits, A. G. Structure−Composition Relationship of Platelike Ferrospheres in Calcium-Rich Power Plant Ash. *Inorg. Mater.* **2018**, *54*, 466−472.
(46) Anshits, N. N.; Fedorchak, M. A.; Zhizhaev, A. M.; Anshits, A. G. A Composition−Structure Relationship of Skeletal-Dendritic Ferrospheres Formed During Industrial Combustion of Lignite and Coal. *Energy Fuels* **2019**, *33*, 6788−6796.
(47) Anshits, N. N.; Fedorchak, M. A.; Zhizhaev, A. M.; Sharonova, O. M.; Anshits, A. G. Composition and Structure of Block-type Ferrospheres Isolated from Calcium-Rich Power Plant Ash. *Inorg. Mater.* **2018**, *54*, 187−194.
(48) Kutchko, B.; Kim, A. Fly ash characterization by SEM−EDS. *Fuel* **2006**, *85*, 2537−2544.
(49) Shpirt, M. Y.; Kler, V. R.; Pertsikov, I. Z. *Inorganic Components of Solid Fuels*; Khimiya: Moscow, 1990. (In Russian).
(50) Vdovchenko, V. S.; Martynova, M. I.; Novitsky, N. V.; Yushina, G. D. *Power fuel in the USSR: handbook*; Energatomizdat: Moscow, 1991. (In Russian).
(51) *Geological dictionary*, 2nd ed.; Puffenholz, K. N., Ed.; Nedra: Moscow, 1978; Vol. 2 (in Russian).
(52) Bryant, G.; Bailey, C.; Wu, H.; McLennan, A.; Stanmore, B.; Wall, T. Iron in Coal and Slagging: The Significance of the High

https://doi.org/10.1021/acsomega.1c02880
ACS Omega 2021, 6, 26004−26015

Temperature Behaviour of Siderite Grains During Combustion. In *Impact of Mineral Impurities in Solid Fuel Combustion*; Gupta, R. P., Wall, T. F., Baxter, L., Eds.; Kluwer Academic/Plenum Publishers: New York, 2002.
(53) Bryers, R. W. Fireside slagging, fouling, and high-temperature corrosion of heat-transfer surface due to impurities in steam-raising fuels. *Prog. Energy Combust. Sci.* **1996**, *22*, 29−120.
(54) Wen, C.; Gao, X.; Xu, M. A CCSEM study on the transformation of included and excluded minerals during coal devolatilization and char combustion. *Fuel* **2016**, *172*, 96−104.
(55) Tectosilicates. Pt. 1: Silicates with interrupted framework, feldspar minerals. In *Minerals: Handbook*; Bokiy, G. B.; Borutzky, B. Y.; Ed.-in-Chiefs, Mozgova, N. N.; Sokolova, M. N., Resp, Eds; Nauka: Moskow, 2003. Vol. *5* (in Russian).
(56) Kalugin, R. A.; Tretyakov, G. A.; Bobrov, V. A. Iron ore basalts in burnt rocks of East Kazakhstan; Trudy Instituta Geologii i Geofiziki, Akademiya Nauk SSSR, Sibirskoe Otdelenie: Novosibirsk, 1991. (In Russian).
(57) Osborn, E. F.; Muan, A. Figure 696. In *Phase Diagrams for Ceramists*; Levin, E. M., Robbins, C. R., McMurdie, H. F., Eds.; American Ceramic Society: Columbus, Ohio, 1964. Vol. *I*.
(58) Sharonova, O. M.; Anshits, N. N.; Anshits, A. G. Composition and morphology of narrowly sized ferrospheres isolated from various types of fly ash. *Inorg. Mater.* **2013**, *49*, 586−594.
(59) Berezhnoi, A. S. *Multicomponent Oxide Systems*; Naukova Dumka: Kiev, 1970. (In Russian).
(60) Esin, O. A.; Gel'd, P. V. *Physical Chemistry of Pyrometallurgical Processes*, 2nd ed.; Part 2; Metallurgiya: Moscow, 1966. (In Russian).
(61) Zhuravlev, G. I. *Chemistry and Technology of Ferrites*; Khimiya: Leningrad, 1970. (In Russian).

https://doi.org/10.1021/acsomega.1c02880
ACS Omega 2021, 6, 26004−26015